

## The Rearrangement Reaction of $\text{CH}_3\text{SNO}_2$ to $\text{CH}_3\text{SONO}$ Studied by a Density Functional Theory Method<sup>†</sup>

Yoon Jeong Choi and Yoon Sup Lee\*

Department of Chemistry, and School of Molecular Science (BK21), Korea Advanced Institute of Science and Technology, Daejeon 305-701, Korea

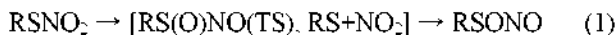
Received May 10, 2004

Several critical geometries associated with the rearrangement of  $\text{CH}_3\text{SNO}_2$  to  $\text{CH}_3\text{SONO}$  are calculated with the density functional theory (DFT) method and compared with those of the *ab initio* molecular orbital methods. There are two probable pathways for this rearrangement, one involving the transition state of an oxygen migration and the other through the homolytic decomposition to radicals. The reaction barrier *via* the transition state is about 60 kcal/mol and the decomposition energy into radicals about 35 kcal/mol, suggesting that the reaction pathway *via* the homolytic cleavage to radical species is energetically favorable. Since even the homolytic cleavage requires large energies, the rearrangement reaction is unlikely without the aid of catalysts.

**Key Words :** Rearrangement reaction of thionitrate, Density functional theory calculations, *Ab initio* MO calculations

### Introduction

The nitric oxide (NO) radical plays an important role in biochemistry and atmospheric chemistry.<sup>1-3</sup> One of reaction pathways proposed earlier involves the initial formation of thionitrate ( $\text{RSNO}_2$ ) as the theoretical source of the NO radical, but the exact function of thionitrate in the biological mechanism of NO is still unresolved despite many experimental and theoretical studies.<sup>4-8</sup> The homolytic decomposition of the sulfenyl nitrite ( $\text{RSONO}$ ), which could be a product of the rearrangement reaction of the thionitrate, was proposed as a possible NO releasing process. This chemically reasonable mechanism is not the major pathway for the formation of the biological NO, but has been the subject of several experimental and theoretical reports.<sup>4,6,9</sup> There are two probable pathways for the rearrangement of  $\text{RSNO}_2$  to  $\text{RSONO}$ , one involving the migration of an oxygen atom and the other through the homolytic cleavage of the S-N bond.



In this work, we study two pathways of the reaction by obtaining optimized geometries of the reactant  $\text{CH}_3\text{SNO}_2$ , the product  $\text{CH}_3\text{SONO}$ , the transition state for oxygen migration in the rearrangement, and radical species in the homolytic decomposition processes using calculations including electron correlations, in part to complement the similar work by Cameron *et al.* on  $\text{HSNO}_2$  and  $\text{CH}_3\text{SNO}_2$ ,<sup>9</sup> which employed somewhat lower levels of calculation in the basis set size and the amount of electron correlations. We analyze the reaction barriers of the two processes in an effort to produce a reliable description of the reaction (1) especially

using the density functional theory (DFT) method. The reaction profile for the  $\text{RSNO}_2$  rearrangement reaction is obtained by the intrinsic reaction coordinate (IRC) analysis.<sup>10</sup> Electron correlations are considered at various levels of the *ab initio* molecular orbital (MO) theory in addition to the DFT method. Sec II briefly outlines the employed basis sets and the quantum chemical methods, followed by results and discussion in Sec III

### Computational Details

The geometries of the reactant  $\text{CH}_3\text{SNO}_2$ , the product  $\text{CH}_3\text{SONO}$  and the transition state of the rearrangement reaction were fully optimized at the Hartree-Fock (HF) and DFT levels of theory. The reaction energies were obtained at the various correlated levels. The reaction path through the calculated transition state was verified by the IRC search.<sup>11,12</sup> Fully optimized geometries of the radical species for the homolytic cleavage were also obtained at the HF and Moller Plesset second order (MP2) levels of theory. In this work, the aqueous solvation energies were not considered. Cameron *et al.*<sup>9</sup> treated solvation energies using the continuum dielectric solvation model (SM3-PM3)<sup>13,14</sup> and the CDM model of Lim and Chan<sup>15</sup> for the aqueous condition, and reported that estimates of the solvation energies differ only slightly (less than 2 kcal/mol) between the thionitrate and sulfenyl nitrite. Thermochemical reaction energies, free energies and enthalpies were obtained from results of Gaussian-1 (G1) and Gaussian-2 (G2) calculations<sup>16-18</sup> as a reference, but most analyses are based upon potential energies without thermal corrections.

DFT calculations were carried out with the PBE1PBE (parameter-free Perdew Burke Ernzerhof's functional)<sup>19</sup> functional. All species of the rearrangement reaction were fully optimized in the DFT calculations employing two

<sup>†</sup>Dedicated to Professor Yong Hae Kim for his distinguished achievements in organic chemistry.

\*Corresponding Author. Fax: +82-42-869-2810; e-mail: yoonsuplee@kaist.ac.kr

different basis sets, 6-311+G\* and 6-311++G\*\*.<sup>20,21</sup> As in the *ab initio* MO calculations, the 6-311+G\* basis set is of the sufficient size for the description of this system since both basis sets affords essentially the same results. Previous works demonstrated that the 6-311++G\*\* basis sets yield a reasonable conformation energy<sup>22</sup> and the PBE1PBE functional produces results in good agreement with the high level correlation treatment of coupled-cluster singles and doubles with perturbed triples [CCSD(T)] for a diatomic molecule.<sup>23</sup> We report values from smaller basis set for MO calculations and those from larger basis set for DFT. All orbitals were included at the MP2 and DFT levels of theory.

All calculations were performed with the Gaussian program package.<sup>24</sup>

## Results and Discussion

The optimized molecular geometries of the reactant CH<sub>3</sub>SNO<sub>2</sub>, the product CH<sub>3</sub>SONO of the rearrangement reaction at the MP2 level of theory and the transition state at the HF level of theory are shown in Figure 1. For the CH<sub>3</sub>SNO<sub>2</sub> molecule, the N-O and N-S bond lengths are increased by 0.04 Å and 0.03 Å, respectively, and the N-S-C angle is decreased by 2° due to electron correlations. For the CH<sub>3</sub>SONO molecule, two N-O bond lengths, one for the terminal O and the other for the connecting O, are also increased by 0.18 Å and 0.02 Å, respectively, and all the bond angles change by less than 1° due to electron correlations. Effects of electron correlations on the geometry are rather small for all structures studied except for the NO distance for the terminal O atom of CH<sub>3</sub>SONO, and the difference between 6-311+G\* and 6-311++G\*\* results are even smaller. The transition state is confirmed by the analysis of vibrational frequencies and the IRC analysis. Figure 1 also describes the reaction paths of the rearrangement through the transition state.

The energies relevant to the rearrangement reaction through the transition state are shown in Table 1. The calculated stabilities of the molecules in the rearrangement

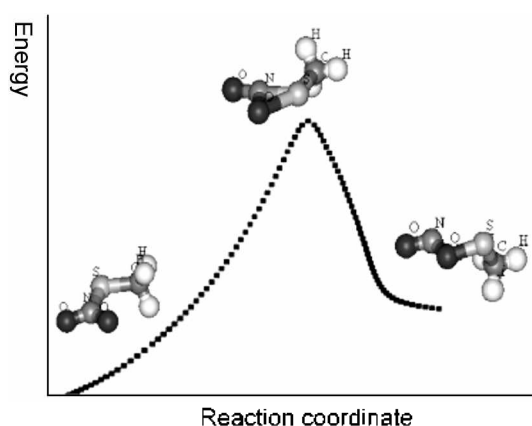


**Figure 1.** The reaction pathway of rearrangement through the transition state analyzed by IRC. The optimized structures for CH<sub>3</sub>SNO<sub>2</sub>, CH<sub>3</sub>SONO and the transition state are also shown.

**Table 1.** Energies (in kcal/mol) of the product CH<sub>3</sub>SONO and the oxygen-migrating transition state relative to the reactant CH<sub>3</sub>SNO<sub>2</sub> at various levels of theory<sup>a</sup>

	$\Delta E$ (P-R) <sup>b</sup>	$\Delta E$ (TS-R) <sup>c</sup>
HF	-0.4	68.0
MP2	12.3	60.9
MP3	5.4	63.9
MP4D	6.0	61.4
MP4DQ	4.4	62.0
MP4SDQ	9.2	53.7
MP4SDTQ	5.2	57.5
CCSD	4.6	58.9
CCSD(T)	6.7	55.5

<sup>a</sup>All energies are single point energies at the HF optimized structures using 6-311+G\* basis sets. <sup>b</sup>Energy difference between the reactant (R) CH<sub>3</sub>SNO<sub>2</sub> and the product (P) CH<sub>3</sub>SONO. <sup>c</sup>Energy difference between the reactant (R) and the transition state (TS).

reaction change drastically upon inclusion of electron correlations. The energy difference between the reactant CH<sub>3</sub>SNO<sub>2</sub> and the product CH<sub>3</sub>SONO is 6.7 kcal/mol and that between the reactant and the transition state 55.5 kcal/mol from the accurate CCSD(T) calculations. In comparison, HF calculations with the same basis set yield -0.4 kcal/mol for the reaction energy and 68.0 kcal/mol for the activation energy. The reaction and activation energies for HSNO<sub>2</sub> obtained by Cameron *et al.*<sup>9</sup> are -1.4 kcal/mol and 55.3 kcal/mol, respectively, at the MP4SDQ/6-31G\* level, while the reaction energy for CH<sub>3</sub>SNO<sub>2</sub> at the same level is 6.0 kcal/mol. The activation energy for CH<sub>3</sub>SNO<sub>2</sub> was not reported by Cameron *et al.*<sup>9</sup> but is likely to be smaller than that of HSNO<sub>2</sub> by about 2 kcal/mol.

The energies of the radical species in the homolytic cleavage are calculated at several levels of theory using restricted (RO-) and unrestricted (U-) open-shell schemes. Cleavage energies deviate substantially at the given level between the two reference schemes although spin contaminations for the unrestricted methods are rather small. The difference between restricted (ROHF and ROMP2) and unrestricted (UHF and UMP2) open-shell values tends to decrease as the amount of electron correlations increases as can be seen from the HF and MP2 results in Table 2. The

**Table 2.** Total energies (in a.u.) and bond dissociation energies ( $D_e$  in kcal/mol) of the homolytic decomposition of CH<sub>3</sub>SNO<sub>2</sub> at various levels of theory<sup>a</sup>

	CH <sub>3</sub> S+NO <sub>2</sub>	CH <sub>3</sub> SNO <sub>2</sub>	$D_e$
UHF	-641.224968	-641.243817	11.8
ROHF	-641.213281	-641.243817	19.2
UMP2	-642.051464	-642.107692	35.3
ROMP2	-642.044614	-642.107692	39.6
ROMP2 <sup>b</sup>	-642.041468	-642.101442	41.6
ROCCSD <sup>b</sup>	-642.057708	-642.115122	36.0
ROCCSD(T) <sup>b</sup>	-642.093146	-642.154161	38.3

<sup>a</sup>All calculations are performed using 6-311+G\* basis sets. <sup>b</sup>Single point energies at the HF-optimized structures.

**Table 3.** Thermochemical energies calculated by G1 and G2 methods for thionitrate and sulphenyl nitrite molecules

	CH <sub>3</sub> SNO <sub>2</sub> (R)	CH <sub>3</sub> SONO (P)	Δ (P-R)
	(in a.u.)	(in a.u.)	(in kcal/mol)
G1 Energy (E)	-642.407649	-642.401707	3.7
G1 Enthalpy (H)	-642.406705	-642.400762	3.7
G1 Free Energy (G)	-642.442790	-642.438101	2.9
G2 Energy (E)	-642.409024	-642.402597	4.0
G2 Enthalpy (H)	-642.408080	-642.401653	4.0
G2 Free Energy (G)	-642.444166	-642.438992	3.2

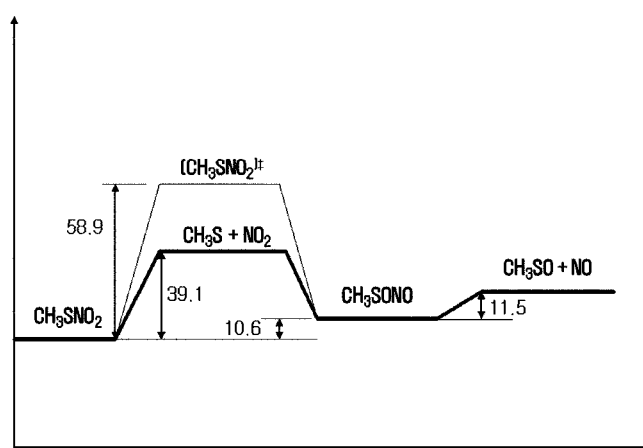
**Table 4.** Total energies E calculated at the PBE1PBE/6-311++G\*\* optimized structures (PBE1PBE/6-311++G\*\*//PBE1PBE/6-311++G\*\*) and the relative energies ΔE (in kcal/mol)

	E (a.u.)	ΔE (kcal/mol)
CH <sub>3</sub> SNO <sub>2</sub> (R)	-642.874781	0.0
CH <sub>3</sub> SONO (P)	-642.856490	11.5
Transition State (TS)	-642.780934	58.9
CH <sub>3</sub> S + NO <sub>2</sub> (Radical 1)	-642.812399	39.1
CH <sub>3</sub> SO + NO (Radical 2)	-642.839602	22.1

unrestricted open-shell reference scheme predicts  $D_0$  to be about 35 kcal/mol at the MP2 level. Since the ROCCSD(T) value at the HF geometry is about the same as the ROMP2 one at the ROMP2 geometry, it is reasonable to estimate  $D_0$  as about 35 kcal/mol. At the highly correlated level, the restricted open-shell scheme may be better, but the unrestricted scheme usually yields values closer to the accurate ones at lower levels of theory.

G1 and G2 calculations which are contrived to include higher order electron correlation corrections of larger basis sets in general<sup>16-18</sup> could give more accurate description of reaction energies. The reaction energies, enthalpies and free energies of the rearrangement from these compounded calculations are shown in Table 3. The reaction energy becomes smaller due to thermal energy corrections to about 4 kcal/mol and the free energy is around 3 kcal/mol.

All structures relevant to the rearrangement reaction are fully optimized using PBE1PBE/6-311++G\*\* calculations. These DFT optimized geometries are in good agreement with those from *ab initio* MO calculations for all the species including the transition state. Total energies and relative energies are listed in Table 4 and Figure 2. Relative energies at the fully optimized geometries using large basis set are close to those of the smaller basis set and also to those estimated by the high-level post-HF calculations at the HF-optimized geometries. The dissociation energy is about 39 kcal/mol and the reaction barrier is close to 60 kcal/mol. The reaction energy for the rearrangement is 11.5 kcal/mol, a value close to the MP2 one. In Table 4, the DFT energy for CH<sub>3</sub>SO+NO is also included and shown to be slightly larger than CH<sub>3</sub>SONO, implying that CH<sub>3</sub>SONO may readily dissociate into those two radicals. The spatial constraint would not allow CH<sub>3</sub>SNO<sub>2</sub> to directly dissociate into

**Figure 2.** Relative energies (in kcal/mol) calculated by the PBE1PBE/6-311++G\*\* method.

CH<sub>3</sub>SO+NO. It is also noted that the stepwise conversion of CH<sub>3</sub>S+NO<sub>2</sub> into CH<sub>3</sub>SO+NO without going through CH<sub>3</sub>ONO requires a large energy to initially separate an O atom from NO<sub>2</sub>. The DFT calculations also confirm that the homolytic cleavage of the SN bond is kinetically most favored reaction in gas phase, and that even this cleavage will require substantial energy. All the calculated values are in reasonable agreement with the G3(MP2) values reported by Wang *et al.*<sup>25</sup> who studied the reaction mechanism of CH<sub>3</sub>S + NO<sub>2</sub> including CH<sub>3</sub>SNO<sub>2</sub> and CH<sub>3</sub>ONO as possible reaction intermediates.

In conclusion, RSNO<sub>2</sub> will require substantial energy in order to rearrange or to decompose in gas phase. A reasonable theoretical treatment of the system should include electron correlations in energy calculations, but the geometry is little affected by the electron correlations. The DFT energies with the PBE1PBE functional appear to be in best agreement with the CCSD ones among the various correlated MO calculations considered for the present case. We do not expect that the inclusion of more dynamic and/or static correlation energy will drastically change the conclusions drawn here. Since one type of RSNO<sub>2</sub> (R = *t*-Butyl) can be readily synthesized<sup>26</sup> and known to produce the NO radical probably *via* RSONO, it may still be worthwhile searching for rearrangement pathways with smaller activation energies.

**Acknowledgement.** Authors are grateful to Prof. Yong Hae Kim for suggesting this topic and helpful discussions for this paper. We would like to dedicate this paper to him in recognition of his great contribution in natural product chemistry and chemical education on the occasion of his official retirement from KAIST. This research is supported by Korea Research Foundation (KRF-2001-015-DS2001) and CNMM of KIMM.

## References

1. Stamler, J. S.; Singel, D. J.; Loscalzo, J. *Science* **1992**, *258*, 1898.
2. Galla, H.-J. *Angew. Chem. Int. Ed. Engl.* **1993**, *23*, 378.
3. Traylor, T. G.; Sharma, V. S. *Biochemistry* **1992**, *31*, 2874.

4. van der Vliet, A.; Hoen, P. A. C.; Wong, P. S.-Y.; Bast, A.; Cross, C. E. *J. Biol. Chem.* **1998**, *273*, 30225.
  5. Feelisch, M. *J. Cardiovasc. Pharmacol.* **1991**, *17*, Suppl. 3, 25.
  6. Artz, J. D.; Yang, K.; Loek, J.; Sanchez, C.; Bennett, B. M.; Thatcher, G. R. *J. Chem. Commun.* **1996**, 927.
  7. Davidson, C.; Kaminski, P.; Wu, M.; Wolin, M. *Am. J. Physiol.* **1996**, *270*, H1038.
  8. Zhang, H.; Squadrito, G.; Uppu, R.; Lemerrier, J.-N.; Cuerto, R.; Pryor, W. *Arch. Biochem. Biophys.* **1997**, *339*, 183.
  9. Cameron, D. R.; Borrajo, A. M. P.; Bennet, B. M.; Thatcher, G. R. *J. Can. J. Chem.* **1995**, *73*, 102.
  10. Fukui, K. *J. Phys. Chem.* **1970**, *74*, 4161.
  11. Gonzalez, C.; Schlegel, H. B. *J. Chem. Phys.* **1989**, *90*, 2154.
  12. Gonzalez, C.; Schlegel, H. B. *J. Chem. Phys.* **1990**, *94*, 5523.
  13. Cramer, C.; Truhlar, D. *J. Comput. Chem.* **1992**, *13*, 1089.
  14. Cramer, C.; Truhler, D. *J. Comput.-Aided Mol. Des.* **1992**, *6*, 629.
  15. Chan, S. L.; Lim, C. *J. Phys. Chem.* **1994**, *98*, 692.
  16. Pople, J. A.; Head-Gordon, M.; Fox, D. J.; Raghavachari, K.; Curtiss, L. A. *J. Chem. Phys.* **1989**, *90*, 5622.
  17. Curtiss, L. A.; Raghavachari, K.; Trucks, G. W.; Pople, J. A. *J. Chem. Phys.* **1990**, *93*, 2537.
  18. Curtiss, L. A.; Raghavachari, K.; Trucks, G. W.; Pople, J. A. *J. Chem. Phys.* **1991**, *94*, 7221.
  19. Adamo, C.; Barone, V. *J. Chem. Phys.* **1998**, *110*, 6158.
  20. McLean, A. D.; Chandler, G. S. *J. Chem. Phys.* **1980**, *72*, 5639.
  21. Krishnan, R.; Binkley, J. S.; Seeger, R.; Pople, J. A. *J. Chem. Phys.* **1980**, *72*, 650.
  22. Han, Y.-K.; Kim, K. H.; Son, S.-K.; Lee, Y. S. *Bull. Korean Chem. Soc.* **2002**, *23*, 1267.
  23. Choi, Y. J.; Bae, C.; Lee, Y. S.; Lee, S. *Bull. Korean Chem. Soc.* **2003**, *24*, 728.
  24. Frisch, M. J. *et al. Gaussian 03 (Revision A.1)*; Gaussian Inc.: Pittsburgh, PA, 2003.
  25. Wang, S. K.; Zhang, Q. Z.; Zhou, J. H.; Gu, Y. S. *Chinese Chem. Lett.* **2002**, *13*, 805.
  26. Oae, S.; Shinhama, K.; Fujimori, K.; Kim, Y. H. *Bull. Chem. Soc. Jpn.* **1980**, 775.
-